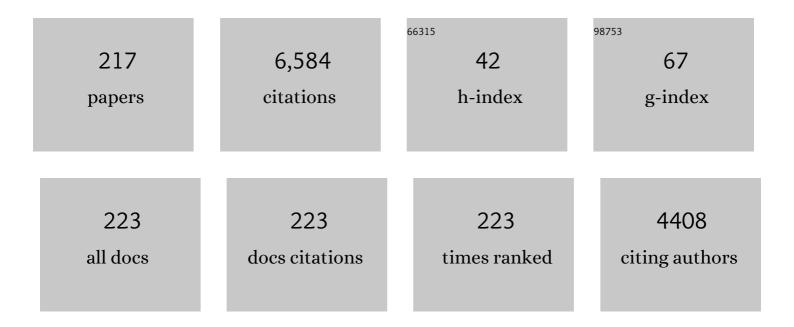
List of Publications by Year in descending order

Source: https://exaly.com/author-pdf/3762601/publications.pdf Version: 2024-02-01



SUK-BONG HONG

#	Article	IF	CITATIONS
1	Hydrothermal stability of CuSSZ13 for reducing NOx by NH3. Journal of Catalysis, 2014, 311, 447-457.	3.1	294
2	Complex zeolite structure solved by combining powder diffraction and electron microscopy. Nature, 2006, 444, 79-81.	13.7	200
3	Catalytic activity of BrĄ̈nsted acid sites in zeolites: Intrinsic activity, rate-limiting step, and influence of the local structure of the acid sites. Journal of Catalysis, 2006, 244, 163-168.	3.1	188
4	A zeolite family with expanding structural complexity and embedded isoreticular structures. Nature, 2015, 524, 74-78.	13.7	167
5	Direct Evidence for the Nonrandom Nature of Al Substitution in Zeolite ZSM-5: An Investigation by 27Al MAS and MQ MAS NMR. Angewandte Chemie - International Edition, 2002, 41, 469-472.	7.2	148
6	Fully Copperâ€Exchanged Highâ€Silica LTA Zeolites as Unrivaled Hydrothermally Stable NH <sub>3</sub> â€SCR Catalysts. Angewandte Chemie - International Edition, 2017, 56, 3256-3260.	7.2	145
7	Effects of cage shape and size of 8-membered ring molecular sieves on their deactivation in methanol-to-olefin (MTO) reactions. Applied Catalysis A: General, 2008, 339, 36-44.	2.2	125
8	Synthesis of High-Silica LTA and UFI Zeolites and NH <sub>3</sub> –SCR Performance of Their Copper-Exchanged Form. ACS Catalysis, 2016, 6, 2443-2447.	5.5	124
9	SAPO-34 and ZSM-5 nanocrystals' size effects on their catalysis of methanol-to-olefin reactions. Applied Catalysis A: General, 2012, 437-438, 120-130.	2.2	121
10	Formation Pathway for LTA Zeolite Crystals Synthesized via a Charge Density Mismatch Approach. Journal of the American Chemical Society, 2013, 135, 2248-2255.	6.6	105
11	Synthesis, Crystal Structure, Characterization, and Catalytic Properties of TNU-9. Journal of the American Chemical Society, 2007, 129, 10870-10885.	6.6	98
12	Influence of framework silicon to aluminium ratio on aluminium coordination and distribution in zeolite Beta investigated by 27Al MAS and 27Al MQ MAS NMR. Physical Chemistry Chemical Physics, 2004, 6, 3031.	1.3	96
13	Synthesis and Characterization of ERI-Type UZM-12 Zeolites and Their Methanol-to-Olefin Performance. Journal of the American Chemical Society, 2010, 132, 12971-12982.	6.6	94
14	Synthesis, Structure Solution, Characterization, and Catalytic Properties of TNU-10:Â A High-Silica Zeolite with the STI Topology. Journal of the American Chemical Society, 2004, 126, 5817-5826.	6.6	93
15	Selective photocatalytic degradation of aquatic pollutants by titania encapsulated into FAU-type zeolites. Journal of Hazardous Materials, 2011, 188, 198-205.	6.5	89
16	Rediscovery of the Importance of Inorganic Synthesis Parameters in the Search for New Zeolites. Accounts of Chemical Research, 2019, 52, 1419-1427.	7.6	82
17	Physicochemical characteristics of pillared interlayered clays. Catalysis Today, 2001, 68, 31-40.	2.2	80
18	Methanol-to-olefin conversion over H-MCM-22 and H-ITQ-2 zeolites. Journal of Catalysis, 2010, 271, 186-194	3.1	80

#	Article	IF	CITATIONS
19	Skeletal isomerization of 1-butene over ferrierite and ZSM-5 zeolites: influence of zeolite acidity. Catalysis Letters, 1996, 36, 249-253.	1.4	73
20	Mechanistic Insights into the Zeolite-Catalyzed Isomerization and Disproportionation of <i>m</i> -Xylene. ACS Catalysis, 2012, 2, 971-981.	5.5	71
21	Characteristics of vanadia on the surface of V2O5/Ti-PILC catalyst for the reduction of NOx by NH3. Applied Catalysis B: Environmental, 2004, 53, 117-126.	10.8	70
22	The Origin of an Unexpected Increase in NH <sub>3</sub> –SCR Activity of Aged Cu-LTA Catalysts. ACS Catalysis, 2017, 7, 6781-6785.	5.5	65
23	Economical synthesis of high-silica LTA zeolites: A step forward in developing a new commercial NH3-SCR catalyst. Applied Catalysis B: Environmental, 2019, 243, 212-219.	10.8	65
24	The Origin of Selective Adsorption of CO <sub>2</sub> on Merlinoite Zeolites. Angewandte Chemie - International Edition, 2021, 60, 4307-4314.	7.2	62
25	Synthesis and Catalytic Behavior of Ferrierite Zeolite Nanoneedles. ACS Catalysis, 2013, 3, 617-621.	5.5	58
26	Reinvestigation into the synthesis of zeolites using diquaternary alkylammonium ions (CH3)3N+(CH2)nN+(CH3)3 with n=3–10 as structure-directing agents. Microporous and Mesoporous Materials, 2004, 68, 97-104.	2.2	56
27	Catalytic evaluation of small-pore molecular sieves with different framework topologies for the synthesis of methylamines. Applied Catalysis A: General, 2006, 305, 70-78.	2.2	56
28	Crystal Structures of Vacuum-Dehydrated Ni <sup>2+</sup> -Exchanged Zeolite Y (FAU, Si/Al = 1.69) Containing Three-Coordinate Ni <sup>2+</sup> , Ni <sub>8</sub> O <sub>4</sub> Â <ii>x</ii> H <sub>2</sub> O <sup>8+</sup> , <iix< ii=""> ≤, Clusters with Near Cubic Ni<sub>4</sub>O<sub>4</sub> Cores, and H<sup>+</sup>. Journal of Physical Chemistry C, 2009, 113, 5164-5181.</iix<>	1.5	56
29	Nature of active sites in Cu-LTA NH3-SCR catalysts: A comparative study with Cu-SSZ-13. Applied Catalysis B: Environmental, 2019, 245, 513-521.	10.8	56
30	Synthesis, characterization, and catalytic properties of zeolites IM-5 andÂNU-88. Journal of Catalysis, 2003, 215, 151-170.	3.1	55
31	Palladium-exchanged small-pore zeolites with different cage systems as methane combustion catalysts. Applied Catalysis B: Environmental, 2017, 219, 155-162.	10.8	51
32	Synthesis of zeolite UZM-35 and catalytic properties of copper-exchanged UZM-35 for ammonia selective catalytic reduction. Applied Catalysis B: Environmental, 2017, 200, 428-438.	10.8	50
33	Zeolite synthesis in the tetraethylammonium–tetramethylammonium mixed-organic additive system. Microporous and Mesoporous Materials, 2009, 123, 160-168.	2.2	48
34	The role of carbonaceous deposits in the skeletal isomerization of 1-butene over ferrierite zeolites. Catalysis Letters, 1996, 41, 189-194.	1.4	47
35	Direct observation of hexamethylbenzenium radical cations generated during zeolite methanol-to-olefin catalysis: an ESR study. Chemical Communications, 2011, 47, 9498.	2.2	46
36	Thermal stability of Pd-containing LaAlO3 perovskite as a modern TWC. Journal of Catalysis, 2015, 330, 71-83.	3.1	46

#	Article	IF	CITATIONS
37	Zeolites ZSM-25 and PST-20: Selective Carbon Dioxide Adsorbents at High Pressures. Journal of Physical Chemistry C, 2017, 121, 3404-3409.	1.5	46
38	In Situ Disorderâ^'Order Transformation in Synthetic Gallosilicate Zeolites with the NAT Topology. Journal of the American Chemical Society, 2004, 126, 13742-13751.	6.6	45
39	A co-templating route to the synthesis of Cu SAPO STA-7, giving an active catalyst for the selective catalytic reduction of NO. Microporous and Mesoporous Materials, 2011, 146, 36-47.	2.2	44
40	Tetramethylbenzenium radical cations as major active intermediates of methanol-to-olefin conversions over phosphorous-modified HZSM-5 zeolites. Journal of Catalysis, 2013, 299, 240-248.	3.1	44
41	Synthesis and Characterization of Gallosilicate Molecular Sieves with High Gallium Contents:Â Examples of Structure Direction Exerted by Gallium. Chemistry of Materials, 2000, 12, 2292-2300.	3.2	43
42	Zeolite synthesis in the presence of flexible diquaternary alkylammonium ions (C2H5)3N+(CH2)nN+(C2H5)3 with n=3–10 as structure-directing agents. Microporous and Mesoporous Materials, 2003, 60, 237-249.	2.2	42
43	Methane Combustion over Pd Catalysts Loaded on Medium and Large Pore Zeolites. Topics in Catalysis, 2009, 52, 27-34.	1.3	41
44	Silicoaluminophosphate Molecular Sieves STA-7 and STA-14 and Their Structure-Dependent Catalytic Performance in the Conversion of Methanol to Olefins. Journal of Physical Chemistry C, 2009, 113, 15731-15741.	1.5	41
45	Unseeded hydroxide-mediated synthesis and CO <sub>2</sub> adsorption properties of an aluminosilicate zeolite with the RTH topology. Journal of Materials Chemistry A, 2015, 3, 19322-19329.	5.2	41
46	Monomolecular Skeletal Isomerization of 1-Butene over Selective Zeolite Catalysts. ACS Catalysis, 2015, 5, 2270-2274.	5.5	41
47	Acidic Properties of Cage-Based, Small-Pore Zeolites with Different Framework Topologies and Their Silicoaluminophosphate Analogues. Journal of Physical Chemistry C, 2011, 115, 22505-22513.	1.5	40
48	Synthesis of Aluminosilicate and Gallosilicate Zeolites via a Charge Density Mismatch Approach and Their Characterization. Journal of the American Chemical Society, 2011, 133, 1917-1934.	6.6	40
49	Effect of Hydrocarbon on DeNOx Performance of Selective Catalytic Reduction by a Combined Reductant over Cu-Containing Zeolite Catalysts. ACS Catalysis, 2019, 9, 9800-9812.	5.5	40
50	Hostâ^'Guest Interactions in Pure-Silica and Aluminosilicate Sodalites Containing Ethylene Glycol as a Guest Molecule. Journal of the American Chemical Society, 1997, 119, 761-770.	6.6	39
51	Zeolite Synthesis from a Charge Density Perspective: The Charge Density Mismatch Synthesis of UZM-5 and UZM-9. Chemistry of Materials, 2014, 26, 6684-6694.	3.2	39
52	Ostwald-ripening sintering kinetics of Pd-based three-way catalyst: Importance of initial particle size of Pd. Chemical Engineering Journal, 2017, 316, 631-644.	6.6	39
53	Framework flexibility-driven CO <sub>2</sub> adsorption on a zeolite. Materials Horizons, 2020, 7, 1528-1532.	6.4	39
54	Synthesis of Zeolite ZSM-57 and Its Catalytic Evaluation for the 1-Butene Skeletal Isomerization and n-Octane Cracking. Journal of Catalysis, 2000, 196, 158-166.	3.1	38

SUK-BONG HONG

#	Article	IF	CITATIONS
55	Zeolite Synthesis Using Flexible Diquaternary Alkylammonium Ions (CnH2n+1)2HN+(CH2)5N+H(CnH2n+1)2withn= 1â^'5 as Structure-Directing Agents. Chemistry of Materials, 2005, 17, 477-486.	3.2	38
56	TNU-7:  A Large-Pore Gallosilicate Zeolite Constructed of Strictly Alternating MOR and MAZ Layers. Chemistry of Materials, 2005, 17, 1272-1274.	3.2	38
57	Comparative catalytic studies on the conversion of 1-butene and n-butane to isobutene over MCM-22 and ITQ-2 zeolites. Journal of Catalysis, 2007, 245, 65-74.	3.1	38
58	CO <sub>2</sub> Adsorption in the RHO Family of Embedded Isoreticular Zeolites. Journal of Physical Chemistry C, 2018, 122, 28815-28824.	1.5	37
59	Iron-substituted TNU-9, TNU-10, and IM-5 zeolites and their steam-activated analogs as catalysts for direct N2O decomposition. Journal of Catalysis, 2011, 284, 23-33.	3.1	36
60	The Origin of Selective Adsorption of CO <sub>2</sub> on Merlinoite Zeolites. Angewandte Chemie, 2021, 133, 4353-4360.	1.6	35
61	PSTâ€1: A Synthetic Smallâ€Pore Zeolite that Selectively Adsorbs H <sub>2</sub> . Angewandte Chemie - International Edition, 2009, 48, 6647-6649.	7.2	33
62	Mechanistic Investigations of Ethylbenzene Disproportionation over Medium-Pore Zeolites with Different Framework Topologies. Journal of Physical Chemistry C, 2011, 115, 16124-16133.	1.5	33
63	Fully Copperâ€Exchanged Highâ€Silica LTA Zeolites as Unrivaled Hydrothermally Stable NH <sub>3</sub> â€SCR Catalysts. Angewandte Chemie, 2017, 129, 3304-3308.	1.6	33
64	A Zeolite Family Nonjointly Built from the 1,3‧tellated Cubic Building Unit. Angewandte Chemie - International Edition, 2018, 57, 2199-2203.	7.2	33
65	Hostâ~'Guest Interactions in P1, SUZ-4, and ZSM-57 Zeolites ContainingN,N,N,Nâ€~,Nâ€~,Nâ€-Hexaethylpentanediammonium Ion as a Guest Molecule. Journal of Physical Chemistry B, 2001, 105, 9994-10000.	1.2	32
66	Influence of Catalytic Functionalities of Zeolites on Product Selectivities in Methanol Conversion. Energy & Fuels, 2009, 23, 593-598.	2.5	32
67	Crystallization Mechanism of Zeolite UZM-5. Chemistry of Materials, 2015, 27, 1574-1582.	3.2	32
68	Synthesis of zeolites P1 and SUZ-4 through a synergy of organic N,N,N,N′,N′,N′-hexaethylpentanediammonium and inorganic cations. Chemical Communications, 2000, , 1609-1610.	2.2	31
69	Molecular Conformations of Protonated Dipropylamine in AlPO4-11, AlPO4-31, SAPO-34, and AlPO4-41 Molecular Sieves. Journal of Physical Chemistry B, 2006, 110, 8188-8193.	1.2	31
70	MSE-Type Zeolites: A Promising Catalyst for the Conversion of Ethene to Propene. ACS Catalysis, 2016, 6, 3870-3874.	5.5	31
71	Synthesis of thermally stable SBT and SBS/SBT intergrowth zeolites. Science, 2021, 373, 104-107.	6.0	31
72	Theoretical Investigation of the Isomerization and Disproportionation of <i>m</i> -Xylene over Medium-Pore Zeolites with Different Framework Topologies. ACS Catalysis, 2014, 4, 1764-1776.	5.5	29

SUK-BONG HONG

#	Article	IF	CITATIONS
73	A quantitative study of the structure–activity relationship in hierarchical zeolites using liquidâ€phase reactions. AICHE Journal, 2019, 65, 1067-1075.	1.8	29
74	Synthesis of microporous gallosilicates with the CGS topology. Journal of Materials Chemistry, 1999, 9, 2287-2289.	6.7	28
75	Tetrahedral Atom Ordering in a Zeolite Framework: A Key Factor Affecting Its Physicochemical Properties. Journal of the American Chemical Society, 2011, 133, 10587-10598.	6.6	28
76	Nitrided ITQ-2 as an efficient Knoevenagel condensation catalyst. Chemical Communications, 2013, 49, 1115.	2.2	28
77	Organicâ€Free Synthesis of Silicoaluminophosphate Molecular Sieves. Angewandte Chemie - International Edition, 2018, 57, 9413-9418.	7.2	28
78	A Zeolite Family Nonjointly Built from the 1,3‣tellated Cubic Building Unit. Angewandte Chemie, 2018, 130, 2221-2225.	1.6	27
79	PST-29: A Missing Member of the RHO family of Embedded Isoreticular Zeolites. Chemistry of Materials, 2018, 30, 6619-6623.	3.2	27
80	Direct N2O decomposition over iron-substituted small-pore zeolites with different pore topologies. Applied Catalysis B: Environmental, 2019, 243, 750-759.	10.8	27
81	Iron-exchanged UZM-35: An active NH3-SCR catalyst at low temperatures. Applied Catalysis B: Environmental, 2020, 266, 118622.	10.8	27
82	Selective catalytic reduction of NO with CH4 over cobalt-exchanged cage-based, small-pore zeolites with different framework structures. Applied Catalysis B: Environmental, 2020, 267, 118710.	10.8	27
83	Distribution and motion of organic guest molecules in zeolites. The Journal of Physical Chemistry, 1993, 97, 1622-1628.	2.9	26
84	Synthesis and characterization of Ga-substituted MER-type zeolites. Microporous and Mesoporous Materials, 2001, 42, 121-129.	2.2	26
85	EUâ€12: A Smallâ€Pore, Highâ€6ilica Zeolite Containing Sinusoidal Eightâ€Ring Channels. Angewandte Chemie - International Edition, 2016, 55, 7369-7373.	7.2	26
86	Targeted Synthesis of Two Superâ€Complex Zeolites with Embedded Isoreticular Structures. Angewandte Chemie - International Edition, 2016, 55, 4928-4932.	7.2	26
87	Crystallization Mechanism of Cage-Based, Small-Pore Molecular Sieves: A Case Study of CHA and LEV Structures. Chemistry of Materials, 2017, 29, 5583-5590.	3.2	26
88	Targeted Synthesis of a Zeolite with Preâ€established Framework Topology. Angewandte Chemie - International Edition, 2019, 58, 13845-13848.	7.2	26
89	Comparative ESR and Catalytic Studies of Ethylene Dimerization on Pd(II)-Exchanged Clinoptilolite, Mordenite, Ferrierite, and SUZ-4. Journal of Physical Chemistry B, 2001, 105, 7730-7738.	1.2	25
90	Use of Flexible Diquaternary Structure-directing Agents in Zeolite Synthesis: Discovery of Zeolites TNU-9 and TNU-10 and Their Catalytic Properties. Catalysis Surveys From Asia, 2008, 12, 131-144.	1.0	25

#	Article	IF	CITATIONS
91	Nanocrystalline beta zeolite: An efficient solid acid catalyst for the liquid-phase degradation of high-density polyethylene. Applied Catalysis B: Environmental, 2008, 83, 160-167.	10.8	25
92	Detailed Determination of the Tl <sup>+</sup> Positions in Zeolite Tlâ^'ZSM-5. Single-Crystal Structures of Fully Dehydrated Tlâ^'ZSM-5 and Hâ^'ZSM-5 (MFI, Si/Al = 29). Additional Evidence for a Nonrandom Distribution of Framework Aluminum. Journal of Physical Chemistry C, 2009, 113, 19937-19956.	1.5	25
93	Hydrocarbon Pool Mechanism of the Zeolite-Catalyzed Conversion of Ethene to Propene. ACS Catalysis, 2019, 9, 10640-10648.	5.5	24
94	Effect of framework Si/Al ratio on the mechanism of CO2 adsorption on the small-pore zeolite gismondine. Chemical Engineering Journal, 2022, 433, 133800.	6.6	24
95	Raman spectra of tetramethylammonium ion-containing molecular sieves. Microporous Materials, 1995, 4, 309-317.	1.6	23
96	Formation of Paramagnetic Defect Centers in Aluminophosphate Molecular Sieves. Journal of the American Chemical Society, 1996, 118, 8102-8110.	6.6	23
97	Synthesis and characterization of a gallosilicate analog of zeolite paulingite. Microporous and Mesoporous Materials, 2005, 83, 319-325.	2.2	23
98	Stability of the Reaction Intermediates of Ethylbenzene Disproportionation over Medium-Pore Zeolites with Different Framework Topologies: A Theoretical Investigation. Journal of Physical Chemistry C, 2013, 117, 23626-23637.	1.5	23
99	An Aluminophosphate Molecular Sieve with 36 Crystallographically Distinct Tetrahedral Sites. Angewandte Chemie - International Edition, 2014, 53, 7480-7483.	7.2	23
100	Si Distribution in Silicoaluminophosphate Molecular Sieves with the LEV Topology:Â A Solid-State NMR Study. Journal of Physical Chemistry B, 2005, 109, 20847-20853.	1.2	22
101	Preparation, Crystal Structure, and Thermal Stability of the Cadmium Sulfide Nanoclusters Cd6S44+and Cd2Na2S4+in the Sodalite Cavities of Zeolite A (LTA). Journal of Physical Chemistry B, 2006, 110, 25964-25974.	1.2	22
102	Silver ZK-5 zeolites for selective ethylene/ethane separation. Separation and Purification Technology, 2020, 250, 117146.	3.9	22
103	Iron-exchanged high-silica LTA zeolites as hydrothermally stable NH <sub>3</sub> -SCR catalysts. Reaction Chemistry and Engineering, 2019, 4, 1050-1058.	1.9	21
104	Structural Chemical Zoning in the Boundary Phase Zeolite TNU-7 (EON). Chemistry of Materials, 2006, 18, 3023-3033.	3.2	20
105	In-situ dehydration studies of fully K-, Rb-, and Cs-exchanged natrolites. American Mineralogist, 2011, 96, 393-401.	0.9	20
106	Zeolite UZM-8: Synthesis, Characterization, and Catalytic Properties in Isopropylation of Benzene with 2-Propanol. Topics in Catalysis, 2015, 58, 537-544.	1.3	20
107	Two Aluminophosphate Molecular Sieves Built from Pairs of Enantiomeric Structural Building Units. Angewandte Chemie - International Edition, 2018, 57, 3727-3732.	7.2	20
108	Water: A promoter of ammonia selective catalytic reduction over copper-exchanged LTA zeolites. Applied Catalysis B: Environmental, 2021, 294, 120244.	10.8	20

#	Article	IF	CITATIONS
109	Skeletal isomerization of 1â€butene on synthetic clinoptilolite zeolite. Catalysis Letters, 1998, 55, 105-112.	1.4	19
110	Probing the non-random aluminum distribution in zeolite merlinoite with ultra-high-field (18.8 T) and MAS NMR. Microporous and Mesoporous Materials, 2002, 52, 55-59.	2.2	19
111	PSTâ€24: A Zeolite with Varying Intracrystalline Channel Dimensionality. Angewandte Chemie - International Edition, 2020, 59, 17691-17696.	7.2	19
112	Synthesis of Zeolite MCM-22 UsingN,N,N,N′,N′,N′-Hexamethyl-1,5-pentanediaminium and Alkali Metal Cations as Structure-directing Agents. Chemistry Letters, 2003, 32, 542-543.	0.7	18
113	Intraframework Migration of Tetrahedral Atoms in a Zeolite. Angewandte Chemie - International Edition, 2014, 53, 8949-8952.	7.2	18
114	Formation and dehydration enthalpies of gallosilicate materials with different framework topologies and Ga contents. Microporous and Mesoporous Materials, 2009, 121, 200-207.	2.2	17
115	Diethylated Diphenylethane Species: Main Reaction Intermediates of Ethylbenzene Disproportionation over Large-Pore Zeolites. Journal of Physical Chemistry C, 2010, 114, 1190-1193.	1.5	17
116	Acid site density effects in zeolite-catalyzed 1-butene skeletal isomerization. Journal of Catalysis, 2016, 335, 58-61.	3.1	17
117	Targeted Synthesis of a Zeolite with Preâ€established Framework Topology. Angewandte Chemie, 2019, 131, 13983-13986.	1.6	17
118	Dehydration of 1,3-butanediol to butadiene over medium-pore zeolites: Another example of reaction intermediate shape selectivity. Applied Catalysis B: Environmental, 2021, 280, 119446.	10.8	17
119	Location of Tb(III) ions in Na-Y zeolite determined by luminescence spectroscopy. Catalysis Letters, 1995, 30, 87-97.	1.4	16
120	Unexpected contraction of a zeolite framework upon isomorphous substitution of Si by Al. Chemical Communications, 1996, , 425.	2.2	16
121	Ammonia IRMS-TPD Characterization of Brà nsted Acid Sites in Medium-pore Zeolites with Different Framework Topologies. Topics in Catalysis, 2010, 53, 664-671.	1.3	16
122	Reaction intermediates and mechanism of the zeolite-catalyzed transalkylation of 1,2,4-trimethylbenzene with toluene. Journal of Catalysis, 2018, 357, 1-11.	3.1	16
123	Molecular Conformation of Hydrogen-Bonded Ethylene Glycol in Sodalite:Â A1H CRAMPS NMR, IR, and2H NMR Study. Journal of Physical Chemistry B, 2002, 106, 6206-6210.	1.2	15
124	Synthesis of Aluminosilicate Natrolites and Control of Their Tetrahedral Atom Ordering. Chemistry of Materials, 2014, 26, 3361-3363.	3.2	15
125	A Family of Molecular Sieves Containing Frameworkâ€Bound Organic Structureâ€Directing Agents. Angewandte Chemie - International Edition, 2015, 54, 11097-11101.	7.2	15
126	Small-pore molecular sieves SAPO-57 and SAPO-59: synthesis, characterization, and catalytic properties in methanol-to-olefins conversion. Catalysis Science and Technology, 2016, 6, 2725-2734.	2.1	15

#	Article	IF	CITATIONS
127	PST-33: A Four-Layer ABC-6 Zeolite with the Stacking Sequence AABC. , 2020, 2, 981-985.		15
128	Effect of preparation method on NH3-SCR activity of Cu-LTA catalysts. Catalysis Today, 2021, 376, 41-46.	2.2	15
129	Double 6-Ring as a Unique Cation Site for the Ce3+/Ce4+Redox Couple in Zeolites. Journal of Physical Chemistry B, 2001, 105, 11961-11963.	1.2	14
130	Influence of Flexibility on the Separation of Chiral Isomers in STW‶ype Zeolite. Chemistry - A European Journal, 2018, 24, 4121-4132.	1.7	14
131	3D-3D topotactic transformation in aluminophosphate molecular sieves and its implication in new zeolite structure generation. Nature Communications, 2020, 11, 3762.	5.8	14
132	Understanding CO2 adsorption in a flexible zeolite through a combination of structural, kinetic and modelling techniques. Separation and Purification Technology, 2021, 256, 117846.	3.9	14
133	Title is missing!. Catalysis Letters, 1999, 57, 179-185.	1.4	13
134	Solid-state NMR evidence for the presence of two crystallographically distinct tetrahedral sites in zeolite merlinoite. Chemical Communications, 2000, , 1719-1720.	2.2	13
135	Structural changes of synthetic paulingite (Na,H-ECR-18) upon dehydration and CO <sub>2</sub> adsorption. Zeitschrift Fur Kristallographie - Crystalline Materials, 2015, 230, 223-231.	0.4	13
136	Charge distribution and conformational stability effects of organic structure-directing agents on zeolite synthesis. Chemical Communications, 2018, 54, 487-490.	2.2	13
137	Colloidal Porous AuAg Alloyed Nanoparticles for Enhanced Photoacoustic Imaging. ACS Applied Materials & Interfaces, 2020, 12, 32270-32277.	4.0	13
138	Electron Spin Resonance and Electron Spin Echo Modulation Studies of Cu(II)-Exchanged Silicoaluminophosphate Type 18 Molecular Sieve. The Journal of Physical Chemistry, 1996, 100, 15954-15960.	2.9	12
139	N,N,N,N′,N′,N′-hexamethylpentanediammonium-MWW layered precursor: A reaction intermediate in the synthesis of zeolites TNU-9 and EU-1. Microporous and Mesoporous Materials, 2009, 124, 227-231.	2.2	12
140	Adsorptive removal of tert-butylmercaptan and tetrahydrothiophene using microporous molecular sieve ETS-10. Applied Catalysis B: Environmental, 2010, 100, 264-270.	10.8	12
141	Microporous aluminophosphates synthesized with 1,2,3-trimethylimidazolium and fluoride. Dalton Transactions, 2016, 45, 7616-7626.	1.6	12
142	Solid solution of a zeolite and a framework-bound OSDA-containing molecular sieve. Chemical Science, 2016, 7, 5805-5814.	3.7	12
143	Charge density mismatch synthesis of zeolite beta in the presence of tetraethylammonium, tetramethylammonium, and sodium ions: Influence of tetraethylammonium decomposition. Microporous and Mesoporous Materials, 2017, 240, 159-168.	2.2	12
144	Conformation of intrazeolitic choline ions and the framework topology of zeolite hosts. Chemical Science, 2018, 9, 7787-7796.	3.7	12

#	Article	IF	CITATIONS
145	Propylene/propane separation on a ferroaluminosilicate levyne zeolite. Microporous and Mesoporous Materials, 2020, 294, 109833.	2.2	12
146	Tetraethylammonium-Mediated Zeolite Synthesis via a Multiple Inorganic Cation Approach. , 2021, 3, 308-312.		12
147	Cupric Ion Species in Cu(II)-Exchanged Kâ^'Offretite Gallosilicate Determined by Electron Spin Resonance and Electron Spin Echo Modulation Spectroscopies. The Journal of Physical Chemistry, 1996, 100, 12624-12630.	2.9	11
148	1,2,4-Trimethylbenzene disproportionation over large-pore zeolites: An experimental and theoretical study. Journal of Catalysis, 2015, 323, 145-157.	3.1	11
149	Synthesis and Structural Characterization of a CHA-type AlPO4 Molecular Sieve with Penta-Coordinated Framework Aluminum Atoms. Inorganic Chemistry, 2017, 56, 8504-8512.	1.9	11
150	Silver-exchanged CHA zeolite as a CO2-resistant adsorbent for N2/O2 separation. Microporous and Mesoporous Materials, 2021, 323, 111239.	2.2	11
151	Solid-state NMR study of various mono- and divalent cation forms of the natural zeolite natrolite. Physical Chemistry Chemical Physics, 2013, 15, 7604.	1.3	10
152	Charge density mismatch synthesis of MEI- and BPH-type zeolites in the TEA <sup>+</sup> –TMA <sup>+</sup> –Li <sup>+</sup> –Sr <sup>2+</sup> mixed-structure-directing agent system. Chemical Communications, 2015, 51, 3671-3673.	2.2	10
153	Modeling short-range substitution order and disorder in crystals: Application to the Ga/Si distribution in a natrolite zeolite. Solid State Nuclear Magnetic Resonance, 2017, 84, 182-195.	1.5	10
154	Stepped Propane Adsorption in Pure-Silica ITW Zeolite. Langmuir, 2018, 34, 4774-4779.	1.6	10
155	Small Gas Adsorption and Separation in Small-Pore Zeolites. Structure and Bonding, 2020, , 1-30.	1.0	10
156	Nanocrystalline Ag-ZK-5 zeolite for selective CH4/N2 separation. Separation and Purification Technology, 2022, 282, 120027.	3.9	10
157	Location and molecular motion of hexamethylbenzene in zeolite NaY. The Journal of Physical Chemistry, 1993, 97, 1629-1633.	2.9	9
158	Copper(II) ionic species in Cull-exchanged K-offretite aluminosilicate and comparison with Cull-exchanged K-offretite gallosilicate determined by electron paramagnetic resonance and electron spin echo modulation spectroscopies. Journal of the Chemical Society, Faraday Transactions, 1997, 93, 1225-1231.	1.7	9
159	Nanocrystalline Hâ€RTH Zeolite: An Efficient Catalyst for the Lowâ€Temperature Dehydration of Ethanol to Ethene. ChemSusChem, 2018, 11, 2035-2039.	3.6	9
160	Combined Alkaliâ€Organoammonium Structure Direction of Highâ€Chargeâ€Density Heteroatomâ€Containing Aluminophosphate Molecular Sieves. Angewandte Chemie - International Edition, 2019, 58, 9032-9037.	7.2	9
161	Dealuminated Cs-ZK-5 zeolite for propylene/propane separation. Chemical Engineering Journal, 2021, 413, 127422.	6.6	9
162	Electron spin resonance studies of O2â^' adsorbed on aluminophosphate molecular sieves. Studies in Surface Science and Catalysis, 1997, 105, 779-786.	1.5	8

#	Article	IF	CITATIONS
163	The physical state of Ga species in Ga-containing mordenite zeolites. Microporous and Mesoporous Materials, 2008, 114, 343-351.	2.2	8
164	Contrasting high-pressure compression behaviors of AlPO4-5 and SSZ-24 with the same AFI framework topology. Microporous and Mesoporous Materials, 2013, 169, 42-46.	2.2	8
165	Framework Al zoning in zeolite ECR-1. Chemical Communications, 2014, 50, 1956.	2.2	8
166	EUâ€12: A Smallâ€Pore, Highâ€Silica Zeolite Containing Sinusoidal Eightâ€Ring Channels. Angewandte Chemie, 2016, 128, 7495-7499.	1.6	8
167	Design of an MWW zeolite catalyst for linear alkylbenzene synthesis with improved catalytic stability. Catalysis Science and Technology, 2016, 6, 2715-2724.	2.1	8
168	Effect of framework Si/Al ratio on the adsorption mechanism of CO2 on small-pore zeolites: II. Merlinoite. Chemical Engineering Journal, 2022, 446, 137100.	6.6	8
169	<i>n</i> -Propylbenzene Disproportionation: An Efficient Tool for Assessing the Framework Topology of Large-Pore Zeolites. Journal of Physical Chemistry C, 2016, 120, 6125-6135.	1.5	7
170	An Aluminosilicate Zeolite Containing Rings of Tetrahedral Atoms with All Odd Numbers from Five to Eleven. Angewandte Chemie - International Edition, 2021, 60, 5936-5940.	7.2	7
171	Preparation and characterization of vanado-, ferri-, and gallosilicate catalysts in the presence of fluoride ions. Korean Journal of Chemical Engineering, 1992, 9, 16-22.	1.2	6
172	EPR and electron spin echo modulation spectroscopy of Cu II ion species in Cu II -exchanged K-L gallosilicate. Journal of the Chemical Society, Faraday Transactions, 1996, 92, 855.	1.7	6
173	Delaminated zeoliteâ€catalysed synthesis of highâ€molecular weight polycarbosilane as a low shrinkage SiC precursor. Journal of Polymer Science Part A, 2008, 46, 725-732.	2.5	6
174	Single Crystal Structure of Zeolite A (LTA) Containing Ag4Cl4Nanoclusters and Reduced 1,3,5-Tripyrylium Dimers with Remarkably Short 2.43 Ã Interplanar Spacings. Journal of Physical Chemistry C, 2008, 112, 11181-11193.	1.5	6
175	Synthesis and in situ transformation of PST-1: a potassium gallosilicate natrolite with a high Ga content. Dalton Transactions, 2010, 39, 2246.	1.6	6
176	Aberration-corrected STEM analysis of the RHO family of zeolites with embedded isoreticular structures. Microporous and Mesoporous Materials, 2016, 236, 129-133.	2.2	6
177	Crystallization Mechanism of a Family of Embedded Isoreticular Zeolites. Journal of Physical Chemistry C, 2017, 121, 16342-16350.	1.5	6
178	Embedded Isoreticular Zeolites: Concept and Beyond. Chemistry - A European Journal, 2017, 23, 15922-15929.	1.7	6
179	Mechanisms for the Reverse Skeletal Isomerization of <i>n</i> â€Butenes to Isobutene over Zeolite Catalysts. ChemCatChem, 2017, 9, 114-116.	1.8	6
180	Synthesis and structure of a CDO zeolite precursor with a high Al content. Inorganic Chemistry Frontiers, 2018, 5, 2792-2797.	3.0	6

11

#	Article	IF	CITATIONS
181	Two Aluminophosphate Molecular Sieves Built from Pairs of Enantiomeric Structural Building Units. Angewandte Chemie, 2018, 130, 3789-3794.	1.6	6
182	Organicâ€Free Synthesis of Silicoaluminophosphate Molecular Sieves. Angewandte Chemie, 2018, 130, 9557-9562.	1.6	6
183	Identifying Crystallographically Different Siâ^'OHâ^'Al BrÃ,nsted Acid Sites in LTA Zeolites. Angewandte Chemie - International Edition, 2022, 61, .	7.2	6
184	Temperature-programmed desorption study of molecular oxygen adsorbed on MFI-type zeolites. Korean Journal of Chemical Engineering, 1998, 15, 566-569.	1.2	5
185	Ammoxidation of isomeric picolines on molybdenum phosphate catalyst. Korean Journal of Chemical Engineering, 2003, 20, 279-283.	1.2	5
186	Effect of CO <sub>2</sub> on the DeNO <sub><i>x</i></sub> Activity of a Small Pore Zeolite Copper Catalyst for NH <sub>3</sub> /SCR. ChemCatChem, 2014, 6, 1186-1189.	1.8	5
187	Structural characterization of various alkali cation forms of synthetic aluminosilicate natrolites. Microporous and Mesoporous Materials, 2015, 210, 20-25.	2.2	5
188	Compositionally Enhanced Flexibility in a Ga-Rich Zeolite Affords Unusual Structural Changes via Alkali Ion Exchange. Chemistry of Materials, 2015, 27, 6177-6180.	3.2	5
189	Extraframework Cation Locations in Cu-UZM-35 NH <sub>3</sub> -SCR Catalyst. Journal of Physical Chemistry C, 2018, 122, 29330-29337.	1.5	5
190	Molecular dynamics and glass-transition of ethylene glycol adsorbed in zeolites: Influence of surface–molecule interactions, topology, and loading degree. Microporous and Mesoporous Materials, 2006, 94, 261-268.	2.2	4
191	Microporous metal–organic framework containing cages with adjustable portal dimensions for adsorptive CO2 separation. RSC Advances, 2012, 2, 11566.	1.7	4
192	Zeolite-Catalyzed Disproportionation of <i>iso</i> -Propylbenzene: Identification of Reaction Intermediates and Mechanism. Journal of Physical Chemistry C, 2016, 120, 11552-11560.	1.5	4
193	Choline-mediated synthesis of zeolite ERS-7 <i>via</i> an excess fluoride approach. Chemical Communications, 2018, 54, 10997-11000.	2.2	4
194	An Aluminosilicate Zeolite Containing Rings of Tetrahedral Atoms with All Odd Numbers from Five to Eleven. Angewandte Chemie, 2021, 133, 6001-6005.	1.6	4
195	Zeolite synthesis by the excess fluoride approach in the presence of piperidinium-based structure-directing agents. Microporous and Mesoporous Materials, 2021, 327, 111422.	2.2	4
196	An intrinsic synthesis parameter governing the crystallization of silico(zinco)aluminophosphate molecular sieves. Chemical Science, 2021, 12, 10371-10379.	3.7	4
197	Culllocation and adsorbate interaction in Cull-exchangedsynthetic Na-omega gallosilicate EPR and electron spin echo modulation studies. Journal of the Chemical Society, Faraday Transactions, 1997, 93, 4211-4219.	1.7	3
198	Thermochemistry of gallosilicate zeolites with the NAT topology: An energetic view on their in situ disorder–order transformation and thermal stability. Microporous and Mesoporous Materials, 2010, 135, 197-200.	2.2	3

#	Article	IF	CITATIONS
199	Synthesis and structural characterization of aluminogermanate pharmacosiderites with different crystal symmetries. Microporous and Mesoporous Materials, 2011, 139, 148-157.	2.2	3
200	Phase Transformation Behavior of a Twoâ€Dimensional Zeolite. Angewandte Chemie - International Edition, 2019, 58, 10230-10235.	7.2	3
201	PSTâ€24: A Zeolite with Varying Intracrystalline Channel Dimensionality. Angewandte Chemie, 2020, 132, 17844-17849.	1.6	3
202	Physicochemical characteristics of Ti-PILC as a catalyst support for the reduction of NO by NH3. Studies in Surface Science and Catalysis, 2003, , 697-700.	1.5	2
203	Targeted Synthesis of Two Superâ€Complex Zeolites with Embedded Isoreticular Structures. Angewandte Chemie, 2016, 128, 5012-5016.	1.6	2
204	Investigations into the Mechanisms of Zeolite-Catalyzed Transalkylation ofiso-Propylbenzene with Toluene. Journal of Physical Chemistry C, 2017, 121, 18057-18064.	1.5	2
205	Abnormal Expansion of a Disordered Zeolite upon Ion Exchange of K <sup>+</sup> by Mg <sup>2+</sup> . Journal of Physical Chemistry C, 2019, 123, 17894-17898.	1.5	2
206	Direct Synthesis of Ge-free IWR-type Zeolites. Chemistry Letters, 2019, 48, 1445-1447.	0.7	2
207	Combined Alkaliâ€Organoammonium Structure Direction of Highâ€Chargeâ€Density Heteroatomâ€Containing Aluminophosphate Molecular Sieves. Angewandte Chemie, 2019, 131, 9130-9135.	1.6	2
208	Transformation Control of a Layered Zeolite Precursor by Simple Cation Exchange. Chemistry of Materials, 2020, 32, 9740-9746.	3.2	2
209	A comparative study of methylamines synthesis over zeolites H-rho and H-PST-29. Microporous and Mesoporous Materials, 2020, 300, 110150.	2.2	2
210	Cupric ion species in Cu(II)-exchanged gallosilicate K-L and comparison with aluminosilicate K-L. Studies in Surface Science and Catalysis, 1997, 105, 801-808.	1.5	1
211	On the Porous Silicate HPMâ€5. European Journal of Inorganic Chemistry, 2017, 2017, 2525-2531.	1.0	1
212	An open-framework silicogermanate regularly constructed from natrolite zeolite chains and Ge <sub>9</sub> O <sub>18</sub> (OH) <sub>4</sub> clusters. Dalton Transactions, 2018, 47, 17122-17126.	1.6	1
213	Phase Transformation Behavior of a Twoâ€Dimensional Zeolite. Angewandte Chemie, 2019, 131, 10336-10341.	1.6	1
214	Effect of alkali metal ions on the intrazeolitic migration of Tb(III) ions in zeolite Y. Reaction Kinetics and Catalysis Letters, 1996, 57, 291-299.	0.6	0
215	Embedded Isoreticular Zeolites: Concept and Beyond. Chemistry - A European Journal, 2017, 23, 15843-15843.	1.7	0
216	Fluoride-free synthesis of high-silica, medium-pore zeolites PST-22 and PST-30. Inorganic Chemistry Frontiers, 0, , .	3.0	0

#	Article	IF	CITATIONS
217	Identifying Crystallographically Different Siâ€OHâ€Al BrÃ,nsted Acid Sites in LTA Zeolites. Angewandte Chemie, 0, , .	1.6	0